JOURNAL OF MATERIALS SCIENCE 27 (1992) 1380–1384

Plasticity of columnar-grained $CoSi_2$ with the C1 structure

S. TAKEUCHI, T. HASHIMOTO
Institute for Solid State Physics, University of Tokyo, Roppongi, Minato-ku, Tokyo 106, Japan

T. SHIBUYA
Faculty of Engineering, Toyo University, Kujirai, Kawagoe-shi, Saitama 350, Japan

Columnar-grained $CoSi_2$ crystals with the C1 structure (CaF_2 type) have been deformed in compression in vacuum at high temperatures up to 1400 K. The yield stress increases steeply with decreasing temperature, and the fracture precedes yielding below 700 K. Above 900 K, specimens can be compressed to a strain above 80% without fracture. From the strain-rate sensitivity determined by the stress relaxation test and the temperature dependence of the yield stress, the activation volume and the activation enthalpy of plastic deformation have been analysed. The activation volumes at high stresses ($\tau^* > 100\ MN\,m^{-2}$) are less than $10\boldsymbol{b}^3$ (where $\boldsymbol{b}$ is the magnitude of the Burgers vector), indicating that the deformation is controlled by the Peierls mechanism. The total activation enthalpy is about 3 eV. The possibility of the dissociation of $1/2\langle 110\rangle$ dislocations is proposed.

1. Introduction

The C1 structure or the fluorite structure (or the anti-fluorite structure) has an fcc crystal symmetry, and hence the crystals with this structure potentially possess a high ductility due to possible activation of a number of slip systems. Among the crystals with this structure, CaF_2 is the only crystal for which plastic properties, such as dislocation mobilities [1, 2], effects of impurities [3, 4], work-hardening characteristics [5] and dislocation structures [6, 7], have been rather extensively investigated. Some other experiments have been reported on dislocation mobilities in BaF_2 [8] and high-temperature plasticity of Li_2O [9]. These crystals are ionic in character and the number of active slip systems in these crystals is limited, probably due to their high ionicity.

Another group of C1 type crystals exists, which are metallic in character. The slip systems in such intermetallic compounds may be different from those of the former group with high ionicity because the dislocation core energy and the stacking fault energy may differ significantly between the two groups. Among the metallic C1 type crystals, silicides such as $NiSi_2$ and $CoSi_2$ are of special interest from the practical point of view, because the layers of these crystals are fabricated on silicon wafers for conduction paths of electronic devices, and also these crystals seem to have potential applications as high-temperature structural material due to their relatively high melting point, high chemical stability and low density. In the present work, we investigated for the first time the high-temperature plasticity of polycrystalline $CoSi_2$; the lattice constant of $CoSi_2$ is 0.5365 nm and the density $4.95\ g\,cm^{-3}$.

2. Experimental procedure

High-purity Co (99.99%) and Si (99.9999%) were arc-melted in an argon atmosphere to produce a button ingot of a stoichiometric $CoSi_2$ crystal. The ingot consisted of columnar grains with a diameter of a few tenths of a millimetre. Rectangular compressive specimens, $2 \times 2 \times 5\ mm^3$ in size, were cut from the ingot. The lengthwise direction or the compressive axis of the specimens was almost parallel to the long direction of the columnar grains. The cross-sectional area perpendicular to the compressive axis contained about 50 grains. The specimens were annealed at 1300 K for 1 h and then polished chemically by the CP4 etchant.

Compressive tests were performed in a vacuum in a tantalum furnace at high temperatures. The strain rate was normally $1.7 \times 10^{-4} s^{-1}$. Temperature-change tests were conducted for some specimens to obtain the temperature dependence of the yield stress; the difference in the yield stress with changing temperature was estimated from the change in the flow stress with temperature change. Stress-relaxation tests were also performed in the initial stage of deformation to obtain the strain-rate sensitivity of the initial flow stress. The instantaneous strain rate during the relaxation process corresponds to the slope of the relaxation curve, and thus the strain-rate sensitivity, $\partial\sigma/\partial\ln\dot{\varepsilon}$ can be estimated approximately from the stress reduction accompanying the slope change by a factor of $e = 2.718$. However, because the work-hardening rate was rather high, we had to take into account the work-hardening contribution to the relaxing stress. Fig. 1 illustrates the method of correcting the relaxation curve by subtracting the work-hardening stress during

0022–2461

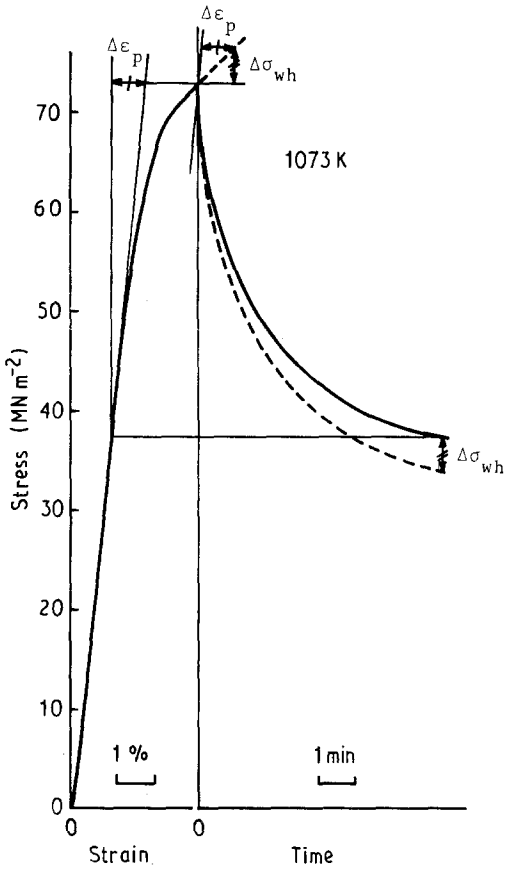

Figure 1 An example of the stress relaxation curve and its correction by taking account of the work-hardening during the relaxation.

the relaxation; $\Delta\varepsilon_p$ and $\Delta\sigma_{wh}$ are the total plastic strain and the total work-hardening stress in the stress–relaxation process.

Using the data of the temperature dependence of the yield stress and those of the strain-rate sensitivity, the activation volume, v^*, and the activation enthalpy of deformation, ΔH, were calculated according to the following equations, assuming the shear stress, τ, on the dislocation motion is one-half the compressive stress.

$$v^* = k_B T\left[\frac{\partial \ln\dot{\gamma}}{\partial\tau}\right]_T = 2k_B T\left[\frac{\partial \ln\dot{\varepsilon}}{\partial\sigma}\right]_T \quad (1)$$

$$\Delta H = -k_B T^2\left[\frac{\partial \ln\dot{\gamma}}{\partial\tau}\right]_T\left[\frac{\partial\tau}{\partial T}\right]_{\dot{\gamma}}$$

$$= -k_B T^2\left[\frac{\partial \ln\dot{\varepsilon}}{\partial\sigma}\right]_T\left[\frac{\partial\sigma}{\partial T}\right]_{\dot{\varepsilon}} \quad (2)$$

3. Results

Fig. 2 shows load–compressive strain curves at four temperatures. Below 700 K, specimens broke before yielding and no appreciable plastic deformation took place. Above 873 K, specimens could be deformed to a very large compressive strain. Fig. 3 shows examples of macrostructures of deformed specimens; the left-hand specimen was deformed to 9% at 1073 K and the right-hand one to 63% at 873 K. It is seen that the deformation was quite uniform along the specimen in a small strain range, but became non-uniform at large

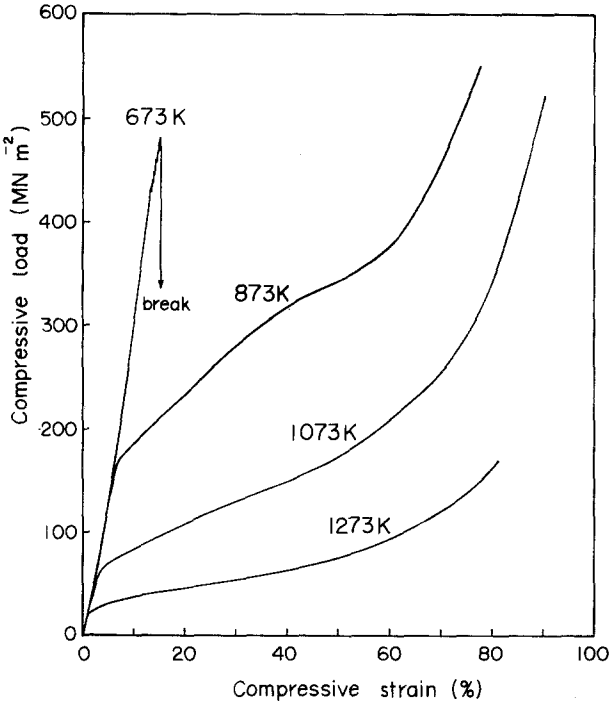

Figure 2 Compressive load–compressive strain curves at various temperatures.

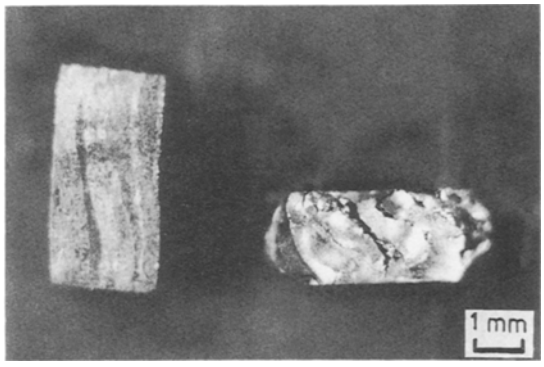

Figure 3 Macro-photographs of compressed specimens: the left-hand specimen was deformed 9% at 1073 K and the right-hand one 63% at 873 K.

strains due to constraint at contact faces, the effect of large grain size and cracking in some cases. Owing to the non-uniform deformation at high strains, we have not attempted to convert the load-compressive curves into true stress–true strain curves.

Strain-rate sensitivity values, estimated from stress relaxation tests performed successively at various strains for the same specimen, are plotted as a function of strain in Fig. 4 for two specimens. It was found that the strain-rate sensitivity values are essentially unchanged with plastic strain, and hence the strain-rate sensitivity value obtained at a small strain may be regarded as the strain-rate sensitivity of the yield stress.

Fig. 5 shows the temperature dependence of the yield stress (b) and that of the strain-rate sensitivity (a). The yield stress increases steeply with decreasing temperature. Similarly, the strain-rate sensitivity increases with decreasing temperature.

Using the data of Fig. 5, activation volumes and activation enthalpies were calculated according to

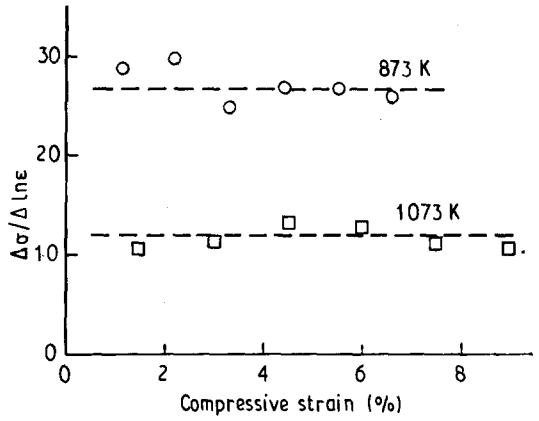

Figure 4 Strain-rate sensitivity values as a function of compressive strain for two temperatures.

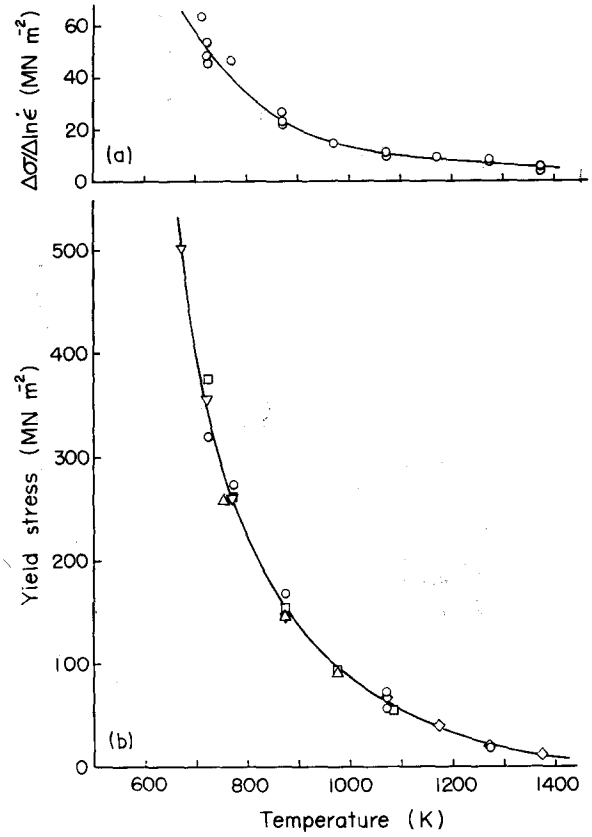

Figure 5 Temperature dependence of (a) strain-rate sensitivity and (b) yield stress. (○) Data for individual specimens; other symbols, data for temperature change tests for the same specimen for each mark.

Equations 1 and 2. Approximating the effective stress as $\tau^* = \sigma_y/2 - 5\ \mathrm{MNm^{-2}}$, we plot in Fig. 6, the activation volumes and the activation enthalpies as a function of the effective stress, τ^*. The activation volume is as small as $10\boldsymbol{b}^3$, where $\boldsymbol{b}$ is the magnitude of the Burgers vector, for τ^* higher than $100\ \mathrm{MNm^{-2}}$. The total activation enthalpy, i.e. the activation enthalpy at zero effective stress, is about 3 eV. The activation enthalpy obtained at each deformation temperature divided by k_BT, i.e. the exponent of the Arrhenius strain-rate equation for a constant strain rate of $1.7 \times 10^{-4}\mathrm{s}^{-1}$, is plotted against temperature in Fig. 7. Although the plots are scattered considerably,

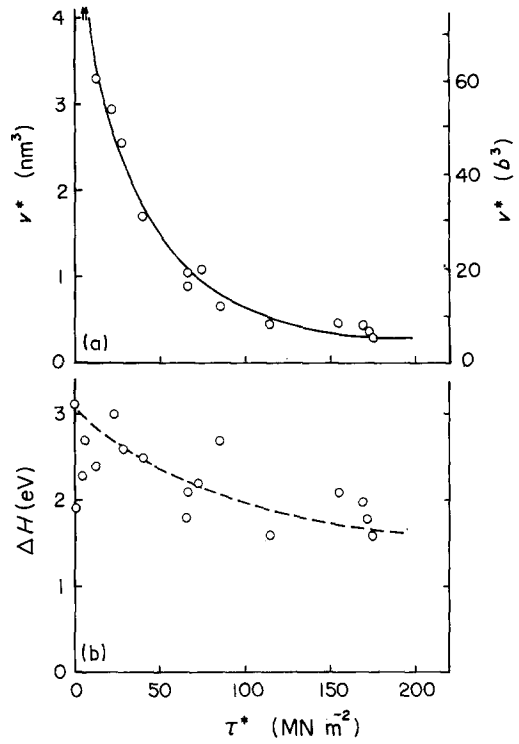

Figure 6 Effective stress dependence of (a) activation volume and (b) activation enthalpy.

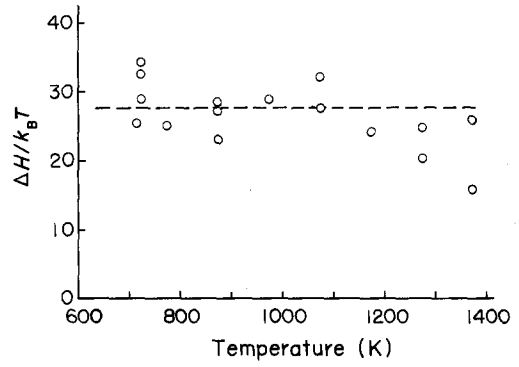

Figure 7 $\Delta H/K_BT$ values for a constant strain rate of $1.7 \times 10^{-4}\mathrm{s}^{-1}$ at various temperatures.

the values are roughly constant around 28, indicating that the Arrhenius rate equation holds approximately.

4. Discussion

The general rule of the activity of the slip system is that the larger the $h/\boldsymbol{b}$ value the higher is the activity, where h is the lattice spacing of the slip plane. This rule is based on the fact that the Peierls potential is the lower for the larger $h/\boldsymbol{b}$ value. The three largest values of $h/\boldsymbol{b}$ in the C1 structure are 0.500, 0.408 and 0.354 for $\{1\,1\,0\}\langle 1\,1\,0\rangle$, $\{1\,1\,1\}\langle 1\,1\,0\rangle$ and $\{0\,0\,1\}\langle 1\,1\,0\rangle$, respectively. In ionic C1 crystals, the primary slip system is $\{0\,0\,1\}\langle 1\,1\,0\rangle$ and the secondary slip system is $\{1\,1\,0\}\langle 1\,1\,0\rangle$ in contradiction with the above rule. Such a discrepancy can often happen in ionic crystals because the electrostatic energy of the dislocation core is another important factor for the stability of the dislocation. Possible atomic configurations with no net charge at the core of primary $1/2[0\,1\,1](1\,0\,0)$

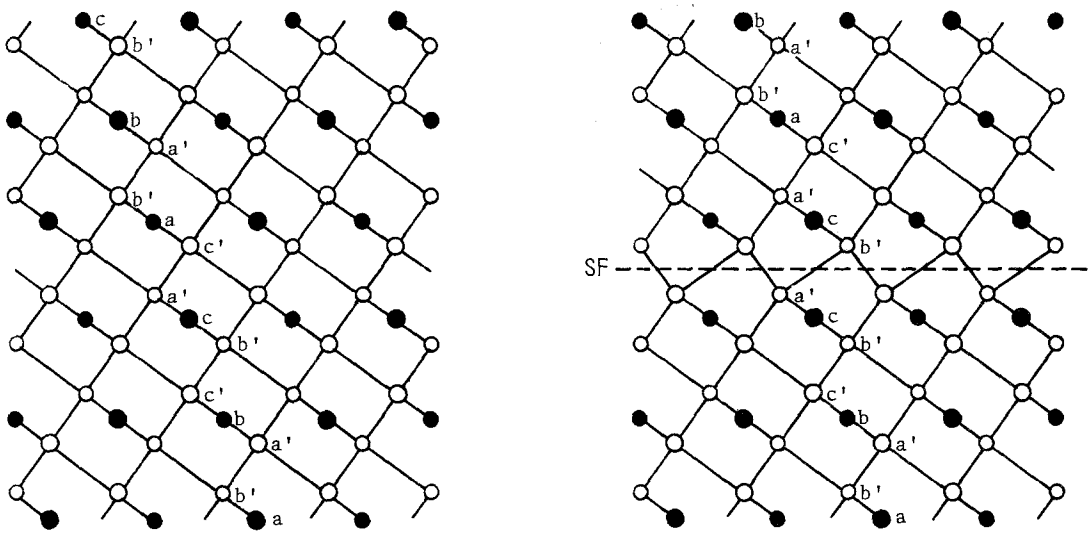

Figure 8 (a) Perfect lattice of the C1 structure viewed from the [110] direction. The vertical direction is [111]. a, b′, a′, b, c′, . . . , indicate the (111) stacking sequence. (○) Si atoms, (●) Co atoms, for $CoSi_2$. The difference in the diameter of the symbols signifies the difference in the positions in the [110] direction. (b) the most probable atomic configuration of the (111) stacking fault with the fault vector of 1/6[211].

dislocation in the C1 structure have been discussed by Evans and Pratt [2].

In metallic materials the above rule is considered to be generally obeyed. If only $\{1\,1\,0\}\langle 1\,1\,0\rangle$ type slip systems with the largest $h/\boldsymbol{b}$ value are active, a large ductility is not expected because among six $\{1\,1\,0\}\langle 1\,1\,0\rangle$ systems only two are independent; for polycrystalline materials to be ductile, at least five independent slip systems are required to be active (the von Mises criterion). Although we have not determined the activated slip systems by direct slip line observation, a preliminary transmission electron microscope observation indicated that dislocations glide on $\{1\,1\,1\}$ planes; thus, the active slip system in $CoSi_2$ appears to be the same as that in elemental fcc metals. This is the origin of the high ductility of the material at high temperatures.

The high activity of $\{1\,1\,1\}\langle 1\,1\,0\rangle$ slip may be due to the dissociation of $1/2\langle 1\,1\,0\rangle$ dislocations on the $\{1\,1\,1\}$ plane according to the same reaction as in elemental fcc metals, i.e. $1/2[1\,1\,0] \rightarrow 1/6[2\,1\,1] + 1/6[1\,2\,\bar{1}]$. After the dissociation, the $h/\boldsymbol{b}_p$ value, where $\boldsymbol{b}_p$ is the magnitude of the Burgers vector of partial dislocations, is 0.612, which is now the largest. The most probable atomic configuration of the stacking fault created by the above dissociation is presented in Fig. 8. The fault energy does not seem to be high from the point of atomic packing, and thus it is highly probable that the fault is stable in metallic C1 crystals, but may not be stable in ionic C1 crystals.

The steep temperature dependence of the yield stress in Fig. 5 and the small activation volume at high stress in Fig. 6 strongly suggest that the deformation is controlled by the Peierls mechanism. From the theory of the Peierls mechanism based on the string model of the dislocation [10], one can obtain the following relation between the Peierls stress, τ_p, and the total activation enthalpy, ΔH_0 [11]

$$\frac{\Delta H_0}{K\boldsymbol{b}^3} \simeq \left[\frac{d}{\boldsymbol{b}}\right]^{\frac{3}{2}}\left[\frac{\tau_p}{K}\right]^{\frac{1}{2}} \qquad (3)$$

where d is the spacing between the Peierls valleys, and K the line tension factor of the dislocation obtained by elastic constants of the crystal. We attempted to obtain τ_p according to Equation 3.

Because no elastic constants data are available for $CoSi_2$ crystal, we roughly estimated Young's modulus of the crystal by a compression test at room temperature; we calculated the Young's modulus from the change of the slope of the load–compression curves with a specimen loaded and without load (blank test). The obtained Young's modulus is 114 GPa. Assuming a Poisson's ratio of 0.3 and isotropic elasticity and using $\Delta H_0 = 3$ eV, $a = 0.5365$ nm, $d = 6^{1/2}a/4$, we estimated τ_p from Equation 3 for the perfect dislocation and the partial dislocation. The results showed that the calculated τ_p is around 2 GPa for the perfect dislocation and 10 GPa for the partial dislocation. It is difficult to extrapolate the $\tau - T$ curve in Fig. 5 to the absolute zero temperature, but we can safely conclude that the extrapolated value is definitely higher than 2 GPa. This means that if the dislocation is not dissociated, the ΔH_0 value and the result of Fig. 5 are inconsistent, whereas they are consistent if the dislocation is dissociated, as discussed above. Attempts to obtain direct evidence for the dissociation by high-resolution electron microscopy are under way.

References

1. G. A. KEIG and R. L. COBLE, *J. Appl. Phys.* **39** (1968) 6090.
2. A. G. EVANS and P. L. PRATT, *Phil. Mag.* **20** (1969) 1213.
3. S. R. SASHITAL and K. VEDAM, *J. Appl. Phys.* **43** (1972) 4396.
4. R. N. KATZ and R. L. COBLE, *ibid.* **45** (1974) 2382.

5. A. G. EVANS and P. L. PRATT, *Phil. Mag.* **21** (1970) 951.
6. W. M. SHERRY and J. B. VANDER SANDE, *Phil. Mag. A* **40** (1979) 77.
7. *Idem, J. Mater. Sci.* **16** (1981) 1477.
8. S. N. VAL'KOVSKII and E. M. NADGORNYI, *Sov. Phys. Solid State* **18** (2) (1976) 320.
9. K. NODA, M. ARITA, Y. ISHII, H. SAKA, T. IMURA, K. KURODA and H. WATANABE, *J. Nucl. Mater.* **141–143** (1986) 353.
10. J. E. DORN and S. RAJNAK, *Trans. Met. Soc. AIME* **230** (1964) 1052.
11. S. TAKEUCHI and T. SUZUKI, in "Strength of Metals and Alloys", edited by P. O. Kettsnen, T. K. Lepisto and M. E. Lehtonen (Pergamon, Oxford, 1988) p. 161.

Received 15 January
and accepted 7 June 1991